EUROPEAN FUSION DEVELOPMENT AGREEMENT

EFDA–JET–CP(01)01-14

M.J. Mantsinen, M.-L. Mayoral, E. Righi, J.-M. Noterdaeme, A.A. Tuccillo, M. de Baar, A. Figueiredo, A. Gondhalekar, T. Hellsten, V. Kiptily, K. Lawson, F. Meo, F. Milani, I. Monakhov, Yu. Petrov, V. Riccardo, F. Rimini, S. Sharapov, D. Van Eester, K.-D. Zastrow, R. Barnsley, L. Bertalot, A. Bickley, J. Bucalossi, R. Cesario, J.M. Chareau, M. Charlet, I. Coffey, S. Conroy, P. de Vries , K. Erents, L.-G. Eriksson, C. Gowers, L.C. Ingesson, N. Jarvis, T. Johnson, R. Koch, Ph. Lamalle, G. Maddison, J. Mailloux, A. Murari, F. Nguyen, J. Ongena, V. Parail ,S. Popovichev, G. Saibene, F. Sartori, J. Strachan, M. Zerbini and Task Force H and JET EFDA contributors

ICRF Heating Scenarios in JET with Emphasis on ^{4}He plasmas for the Non-activated Phase of ITER

ICRF Heating Scenarios in JET with Emphasis on ^{4}He plasmas for the Non-activated Phase of ITER

M.J. Mantsinen[1], M.-L. Mayoral[2], E. Righi[3], J.-M. Noterdaeme[4], A.A. Tuccillo[5], M. de Baar[6], A. Figueiredo[7], A. Gondhalekar[2], T. Hellsten[8, 9], V. Kiptily[2], K. Lawson[2], F. Meo[4], F. Milani[2], I. Monakhov[2], Yu. Petrov[10], V. Riccardo[2], F. Rimini[11], S. Sharapov[2], D. Van Eester[12], K.-D. Zastrow[2], R. Barnsley[2], L. Bertalot[11], A. Bickley[2], J. Bucalossi[11], R. Cesario[5], J.M. Chareau[11], M. Charlet[2], I. Coffey[2], S. Conroy[8], P. de Vries[6], K. Erents[2], L.-G. Eriksson[11], C. Gowers[2], L.C. Ingesson[6], N. Jarvis[2], T. Johnson[8], R. Koch[12], Ph. Lamalle[9, 12], G. Maddison[2], J. Mailloux[2], A. Murari[5], F. Nguyen[11], J. Ongena[12], V. Parail[2], S. Popovichev[2], G. Saibene[3], F. Sartori[2], J. Strachan[13], M. Zerbini[5] and Task Force H and JET EFDA contributors*

E[1]Helsinki Univ. of Technology, Association Euratom-Tekes, P.O.Box 2200, FIN-02015 HUT, Finland

[2]Association Euratom-UKAEA, Culham Science Centre, Abingdon OX14 3DB, UK

[3]EFDA CSU-Garching, Boltzmann-Str.2, D-85748 Garching, Germany

[4]Max-Planck IPP-EURATOM Assoziation, Boltzmann-Str.2, D-85748 Garching, Germany

[5]Associazione EURATOM-ENEA sulla Fusione, CR Frascati, C.P. 65, 00044 Frascati, Rome, Italy

[6]FOM-Rijnhuizen, Ass. Euratom-FOM, TEC, PO Box 1207, 3430 BE Nieuwegein, NL

[7]Associação EURATOM-IST, Centro de Fusão Nuclear, 1049-001 Lisboa, Portugal

[8]Euratom-VR Association, Swedish Research Council, SE 10378 Stockholm, Sweden

[9]EFDA-JET CSU, Culham Science Centre, Abingdon OX14 3DB, UK

[10]Prairie View A&M University, Prairie View, 77446, USA

[11]Association EURATOM-CEA, CEA-Cadarache, 13108 Saint-Paul-Lez Durance, France

[12]LPP-ERM/KMS, Association Euratom-Belgian State, TEC, B-1000 Brussels, Belgium

13Princeton Plasma Physics Laboratory, Princeton, New Jersey 08543, USA

** See annex of J. Pamela et al, "Overview of Recent JET Results and Future Perspectives", Fusion Energy 2000 (Proc. 18th Int. Conf. Sorrento, 2000), IAEA, Vienna (2001).*

Preprint of Paper to be submitted for publication in Proceedings of the
14th APS Topical RF Conference,
(Oxnard, C.A., USA 7-9 May 2001)

‘‘This document is intended for publication in the open literature. It is made available on the understanding that it may not be further circulated and extracts or references may not be published prior to publication of the original when applicable, or without the consent of the Publications Officer, EFDA, Culham Science Centre, Abingdon, Oxon, OX14 3DB, UK.”

“Enquiries about Copyright and reproduction should be addressed to the Publications Officer, EFDA, Culham Science Centre, Abingdon, Oxon, OX14 3DB, UK.”

ABSTRACT

Abstract In the initial phase of ITER operation, ^{4}He plasmas could be used in order to avoid activating the machine. The main ICRH scenarios foreseen for ITER ^{4}He plasmas are (^{3}He) ^{4}He and (H) ^{4}He. ICRH experiments have been carried out on JET using ^{4}He plasmas to validate these scenarios. At the same time, conditions for access to H-mode in plasmas of various isotope compositions from dominantly ^{4}He to dominantly D have been studied. Experiments have also been carried out for the first time in ^{4}He plasmas with the ICRF power added to ^{4}He neutral beam injection at the third harmonic of ^{4}He in order to produce a ^{4}He tail for alpha particle studies.

1. INTRODUCTION

Heating with electromagnetic waves in the ion cyclotron range of frequencies (ICRF) is a well-established method for auxiliary heating of present-day tokamak plasmas and is envisaged as one of the main heating techniques for the International Thermonuclear Experimental Reactor (ITER) and future reactor plasmas. ICRF heating scenarios to be used in ITER D-T plasmas have been studied in detail on TFTR [1,2] and JET [3,4]. For the initial non-activated phase of ITER, H plasmas are at present envisaged. A disadvantage of H plasmas is, however, that twice as much power as in D plasmas is required for access to the H-mode [5]. Alternatively, ^{4}He plasmas could be used in order not to activate the machine. The main ICRF heating scenarios foreseen for ITER ^{4}He plasmas are:

(a) (H)^{4}He, which is the most promising ITER scenario in ^{4}He, covering a magnetic field B range of 3–5T

(b) (^{3}He)^{4}He, which is important for ITER at higher B, e.g. at 5.3T.

Here, the standard notation giving minority species in the parenthesis followed by majority ion species is used. These scenarios are unusual and the experimental database rather limited. In order to validate them ICRF heating experiments have been carried out on JET using ^{4}He plasmas. A large number of new ICRF physics results were obtained with the (^{3}He) ^{4}He scenario which was studied systematically for the first time on JET, by scanning the ^{3}He concentration from the ^{3}He minority heating regime to the mode conversion (MC) regime. Direct comparisons were made with experiments in D plasmas. Heating efficiencies of various scenarios (minority ^{3}He, minority H, and second harmonic H) in ^{4}He were assessed and found to be similar to those in D. All these scenarios triggered an H-mode. Preliminary analysis based on these pulses shows that the L-H mode power threshold is about 65% higher in ^{4}He than in D. Experiments were also carried out for the first time in ^{4}He plasmas with ICRF power added to ^{4}He neutral beam injection (NBI) at the third harmonic of ^{4}He. The aim of these experiments was to produce a ^{4}He tail for alpha particle studies. The results from these experiments are reviewed, including evidence for an alpha tail, competing absorption mechanisms and excitation of Alfvén eigenmodes. Although alpha particles in these experiments are not fusion-born, they form a good starting point for further experiments on alpha particle effects, in view of alpha particle studies in D-T plasmas.

2. (^{3}HE) ^{4}HE AND (^{3}HE)D SCENARIOS

The (^{3}He)4 He and (^{3}He)D scenarios were studied systematically by scanning the ^{3}He concentration using ^{3}He puffs from the ^{3}He minority heating regime to the MC regime. These experiments were carried out in L mode plasmas with B at the plasma centre in the range of 3.45-3.7T and with an ICRF frequency of 34 or 37MHz. A number of new ICRF physics results were obtained, including the first direct evidence for the ICRF-induced pinch of the resonating ions [6,7] at low ^{3}He concentrations and the first detailed assessment of the MC regime on JET at higher ^{3}He concentrations.

3. DIRECT EVIDENCE FOR ICRF-INDUCED PINCH OF ^{3}HE MINORITY IONS

The ICRF-induced pinch [6,7] arises due to the change in toroidal momentum a trapped ion undergoes when interacting with the magnetosonic wave, resulting in a shift in the radial positions of the turning points of its orbit. If toroidally asymmetric ICRF waves are used, the resulting spatial pinch of the trapped ions is either inwards or outwards depending on the toroidal direction in which the launched wave propagates. Earlier, indirect evidence of ICRF-induced pinch of hydrogen minority ions has been obtained on JET based on differences in the sawteeth behaviour, line-integrated proton distribution functions and Alfvén eigenmode activity [6]. In the present experiments, the radial profile of fast ^{3}He ions was measured directly during high power ^{3}He minority heating with a gamma emission profile monitor [8]. This diagnostic is sensitive to gamma ray emission in the energy range of 1.8-6 MeV; the main reaction giving rise to gamma rays in the present experiments is ^{12}C(^{3}He, pγ) ^{14}N.

Figure 1 shows the radial extent of the gamma ray emission at its half maximum as measured with the gamma emission profile monitor in two 3.45T/1.8MA discharges. In both discharges 7MW of ICRF power was tuned to a central ^{3}He minority resonance with $n(^3\mathrm{He})/n_e \approx$ 1-2%, but in one discharge the waves were launched in the co-current direction (+90^o phasing) while in the other discharge the waves were in the counter-current direction (-90^o phasing). The radial extent of the gamma ray emission for -90^o phasing is about 50% wider than for +90^o phasing, clearly indicating that the radial profile of fast ^{3}He ions is more peaked with +90^o phasing. The emission for +90^o phasing is shifted to the low field side, as expected for inward pinch that can produce non-standard passing particles on the low field side [7]. Further confirmation is obtained from sawteeth and excitation of Alfvén eigenmodes (AEs) as in earlier H minority experiments [6]. With +90^o phasing toroidal and elliptical AEs were observed for the first time during ^{3}He minority heating on JET. Here, it should be noted that the excitation of AEs by energetic ions is easier in ^{4}He than in standard D plasmas. This is because for a given electron density and ion temperature, the ratio of the Alfvén velocity to the thermal velocity of ions is higher in ^{4}He than in D, giving rise to a smaller damping rate of Alfvén waves due to thermal ions in ^{4}He. With -90^o phasing, no signs of AEs were observed. From the measurements of diamagnetic energy content (W_{DIA}) and background plasma density and temperature, the perpendicular fast ion energy content, $W_{\perp,fast}$, is estimated to be about 0.5 and 0.3MJ with +90^o and -90^o phasings, respectively. Furthermore, analysis of gamma ray spectra [9] gives a ^{3}He tail temperature of about 0.65 and 0.5MeV with +90^o and -90^o phasings, respectively. Simulations with the SELFO code [10] confirm that these

observations are consistent with the ICRF-induced pinch of ^{3}He minority ions as predicted by theory [6,7].

4. ASSESSMENT OF THE MODE CONVERSION REGIME

As $n(^3\text{He})/n_e$ was increased with ^{3}He puffs from 1-2% to the range of 20%, the ^{3}He tail was observed to diminish and finally disappear using gamma ray emission spectroscopy [9], as expected. The direct electron power deposition was deduced by Fourier and break-in-slope analysis of fast spatially-resolved ECE electron temperature data during ICRF power modulation; the two methods gave similar results. With increasing ^{3}He puff, a transition from a rather broad central to more peaked off-axis direct electron power deposition was observed, as expected (Fig.2). In these 3.45T/1.8MA discharges, ICRF power, applied with a frequency of 37MHz to place the ^{3}He resonance on the HFS at 2.8m, was square-wave modulated with amplitude of 50% and frequency of 20Hz. Modulation of T_e due to direct electron power deposition is caused by the MC layer on the same flux surface on the high-field side and by direct electron damping of the fast wave in the plasma centre. By integrating the measured direct electron deposition profile over the volume, a lower estimate for direct electron damping is obtained due to e.g. the finite spatial coverage of T_e measurements. For discharges in Fig.2 direct electron damping thus obtained increases from 15 to 70% of the launched ICRF power when moving from central to most off-axis deposition.

With the ^{3}He resonance layer inside or close (i.e. within 10cm) to the q=1 surface, the character of sawteeth changed from discharge to discharge as ^{3}He puff before the application of ICRF power was increased. At low ^{3}He puff ($<4\times10^{20}$ el), sawteeth were stabilised by fast ^{3}He ions. With increasing ^{3}He puff (5 to 14×10^{20} el), sawtooth stabilisation took place later in time, preceded by 'normal' sawteeth. These results appear to be consistent with a transition from the MC regime to the ^{3}He minority regime as the ^{3}He concentration in the discharge decays in time, resulting in an increase in the fast ion pressure inside the $q = 1$ surface. At high ^{3}He puff of 18×10^{20} el, sawteeth disappeared. By continuous ^{3}He puffing during ICRF heating, it was possible to keep the off-axis power deposition constant in time, thus demonstrating the controllability of the MC regime (Fig.3). Here, a lower estimate for direct electron damping of 50-60% of the launched ICRF power is obtained by integrating the measured deposition profile over the volume. With a target Te increased from 3.5keV to 4.5keV by 3MW of LHCD power, the off-axis MC power deposition profile was found to broaden. Generally, -90^o, $+90^o$ and dipole phasings were found to give rise to similar power deposition profiles in the MC regime, with somewhat higher direct electron power densities in the early part of the discharge with -90^o phasing. A central T_e in excess of 8keV for $n_e(0) = 3\times10^{19}$ m^{-3} was obtained with 5 MW of ICRF power with central MC.

Surprisingly, gamma ray, high-energy neutral-particle analyser (NPA) [11], and neutron emission measurements indicate D and ^{3}He tails at highest ^{3}He puffs in D plasma in the presence of diagnostic D beams, with stronger D tails for a more central D cyclotron resonance layer. The NPA measurements clearly show that the D distribution functions extend into the MeV range. The maximum neutron

emissivity is localised on the high field side of the torus, close to the D ion cyclotron resonance layer. These observations are similar to those reported from MC experiments on TFTR [12]. A possible explanation could be that above the optimum ^{3}He concentration for MC, the wave field becomes strong with a large $|E_-/E_+|$ ratio due to the shielding of the E_+ component [7]. In such conditions ion damping of the fast wave, dominated by the E_- component, is analogous to third harmonic damping [7]. It possible that knock-on effects play a role to enhance D damping.

Preliminary calculations of MC, based on coupling of the full-wave ALCYON code and the ray-tracing RAYS code [13], for the discharge in Fig.3 indicate comparable direct electron power deposition profiles (Fig.4) to those measured (Fig.3b). For the chosen toroidal mode number N=14, which represents the maximum of antenna power spectrum, the phase velocity of the waves in the MC layer is close to the electron thermal velocity, giving rise to strong electron damping in the immediate vicinity of the layer. In these conditions the IBW rays evolution does not lead to significant modification of the power deposition and the broadening of the direct electron damping profile is mainly due to the vertical extent of the MC layer. The ratio of the calculated ^{3}He ion to electron power deposition is about 10%.

5. HEATING EFFICIENCY AND ACCESS TO H-MODE

The overall heating efficiencies of the (^{3}He) ^{4}He and (H) ^{4}He scenarios were found to be similar to those of the (^{3}He)D and (H)D scenarios, respectively. Using hydrogen minority heating the heating efficiency of monopole (0000) phasing was found to be poorer than the usual dipole (0π0π) phasing and the heating efficiency of 00ππ phasing is between those of monopole and dipole phasings, as in D [14]. The conditions for access to H-mode in plasmas of various isotope compositions from dominantly ^{4}He to dominantly D were studied for several scenarios (minority H, minority ^{3}He, and second harmonic H). All these scenarios triggered the H-mode, while the L-H power threshold was found to be about 65 % higher in ^{4}He than in D.

6. THIRD HARMONIC HEATING OF ^{4}HE

Experiments in ^{4}He plasmas with ICRF power added to ^{4}He NBI at the third harmonic of ^{4}He aimed at producing a ^{4}He tail for alpha particle studies. Particular attention was given to the detection of the alpha tail and its effects on the plasma, such as electron heating, sawtooth stabilisation and excitation of Alfvén eigenmodes. The experiments turned out to be more complicated than anticipated to analyse due to the presence of an energetic deuterium population, indicating that some ICRF power was absorbed at the third harmonic D resonance (typically, n(D)/[n(D)+n(^{4}He)] was about 0.2). However, by optimal use of the NBI system, i.e. by using the highest energy beams with the most central deposition, it was possible to obtain clear evidence for a significant alpha tail and its effects on the plasma.

An overview of two discharges, one with 2MW of 70keV ^{4}He beams and other with 1.5MW of 120keV ^{4}He beams is shown in Fig.5a. As can be seen, W_{DIA} and T_e are higher, R_{NT} is smaller, and

sawteeth are stabilised when 120keV beams are used. Furthermore, the discharge with 120keV beams goes to H-mode while the other discharge stays in L mode. With 70 and 120keV beams, we estimate that about 50% and 85% of the input ICRF power, respectively, is absorbed in the main plasma. At the application of ICRF power, the rise of R_{NT} starts later in time than that of W_{DIA} and T_e, indicating that it takes some time for D damping to develop in the presence of other central damping mechanisms, i.e. ^{4}He damping and direct electron damping. The fast-ion energy content $W_{\perp fast}$ is about 0.25 and 0.6MJ with 70 and 120keV beams, respectively. Note also that not only W_{DIA} but also R_{NT} decay after NBI is switched off.

Gamma ray spectra recorded in the discharges are shown in Fig.5b. Details of the spectra reveal that, when the beam energy is increased from 70 to 120keV, the number of 2MeV alphas, giving rise to gamma ray emission due to the reaction ^{9}Be(α, nγ) ^{12}C [15], increases and the number of the fast D ions decreases while their energy increases. In a subsequent discharge with half the ICRF power and 1.5MW of 120keV beams, the D tail disappears but the ^{4}He tail is visible, but significantly smaller. In another discharge without ^{4}He beams, neither fast deuterons nor fast ^{4}He are observed in the gamma ray spectrum.

In discharge with 120keV beams in Fig.5, magnetic pick-up coils at the plasma edge register multiple elliptical AEs in the frequency range of 400kHz. The EAEs have dominant toroidal mode numbers $n = 5$ and $n = 6$ and are centrally located around r/a •0.3-0.6. They appear at $t = 19.5$s before any significant increase in R_{NT}. Thus, these modes are likely to be driven by energetic ^{4}He ions and thereby constitute the first observations of AEs excited by alpha particles (although not fusion born) on JET. In discharge with 70keV, no such modes are observed.

The experiments have been modelled with the PION code, with the same physics assumptions as used for modelling of earlier third harmonic D heating experiments in JET [16]. According to PION simulations, ^{4}He damping dominates over D and direct electron damping, and D absorption of < 1MW is sufficient to give rise to the measured relatively low neutron rates. To explain details of the observed neutron rates, it appears possible that D damping is enhanced by knock-on collisions between thermal deuterons and fast ^{4}He ions.

ACKNOWLEDGEMENTS

This work has been performed under the European Fusion Development Agreement.

REFERENCES

[1]. Phillips, C.K., et al., Phys. Plasmas **2**, 2427 (1995).

[2]. McGuire, K.M., et al., Phys. Plasmas **2**, 2176 (1995).

[3]. Start, D.F.H., et al., Nuclear Fusion **39**, 321 (1999).

[4]. Start, D.F.H., et al., Phys. Rev. Lett. **80**,4681 (1998).

[5]. Righi, E., et al., Nuclear Fusion **39**, 309 (1999)

[6]. Eriksson, L.-G., et al., Phys. Rev. Lett. **81**, 1231 (1998).

[7]. Hellsten, T., et al., this conference

[8]. Adams, J.M., et al., Nucl. Instrum. Methods Phys. Res., Sect A **329**, 277 (1993).

[9]. Sadler, G.J., et al., Fusion Techn. **18**, 556 (1990).

[10]. Johnson, T., et al., "RF-induced pinch of resonating 3 He minority ions in JET," this conference.

[11]. Korotkov, A.A., Gondhalekar, A., and Stuart, A.J., Nuclear Fusion **33**, 35 (1997).

[12]. Darrow, D.S., et al., Nuclear Fusion **36**, 509 (1996).

[13]. Petrov Yu., et al., Phys. Plasmas **7**, 911 (2000).

[14]. Tuccillo, A.A., et al., this conference.

[15]. Kiptily V.G., Fusion Techn. **18**, 583 (1990).

[16]. Eriksson, L.-G., et al., Nuclear Fusion **38**, 265 (1998).

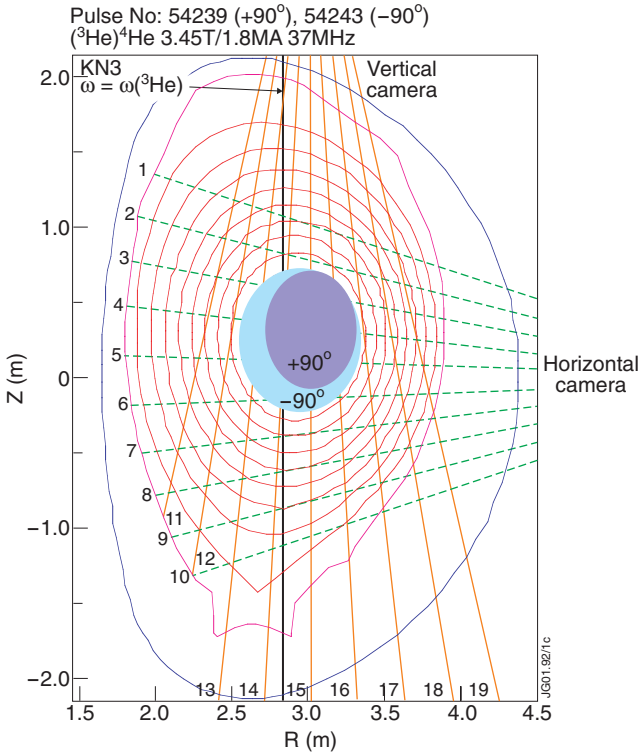

Figure 1: Radial extent of gamma ray emission at its half maximum as measured with the gamma emission profile monitor for the two discharges, deposition one with $+90^{o}$ and the other with -90^{o} phasing.

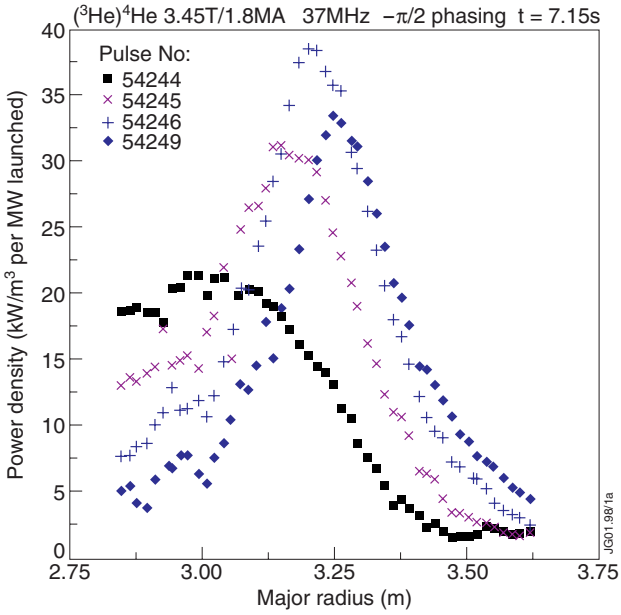

Figure 2: With increasing ^{3}He puff, transition from central to off-axis direct electron power is observed with the break-in-slope analysis of T_e data during ICRF power modulation.

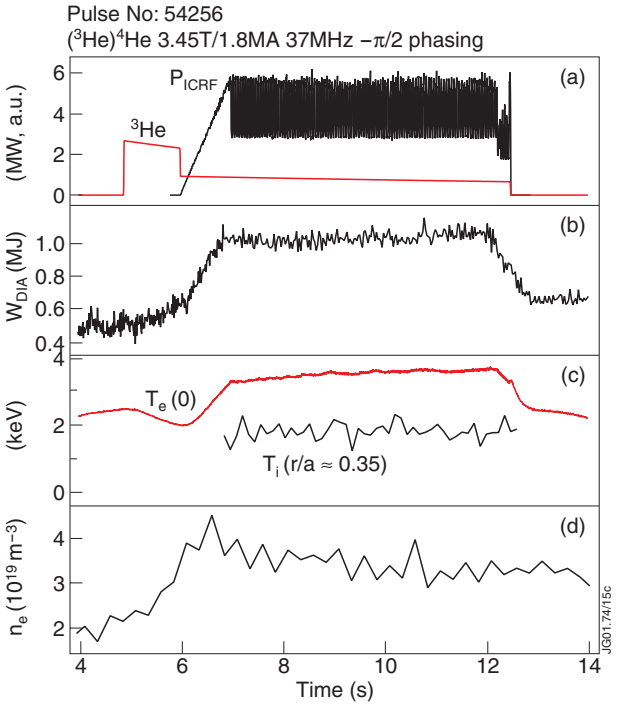

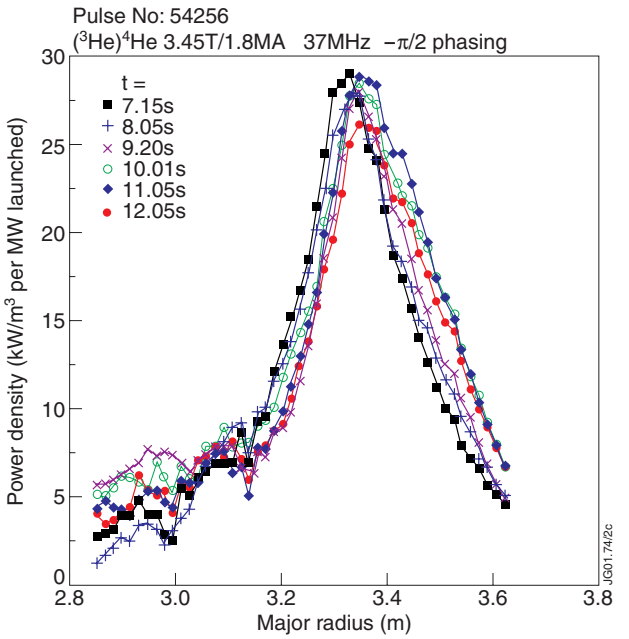

Figure 3: (a) Overview of a discharge with continuous ^{3}He puffing during ICRF heating in order to keep the off-axis direct electron power deposition constant in time as shown in (b).

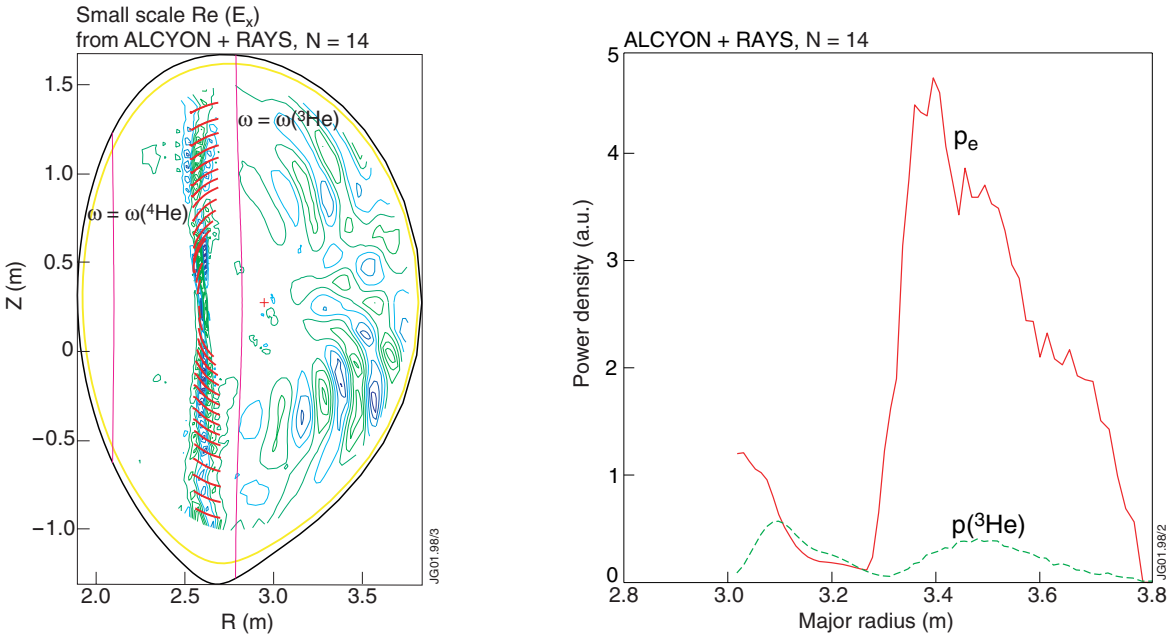

Figure 4: (a) Small-scale RF electric field E pattern extracted from ALCYON global solution with superimposed IBW rays trajectories. (b) Calculated power deposition profiles as given by ALCYON+RAYS (N = 14), mirrored vs magnetic axis to facilitate the comparison with experimental data.

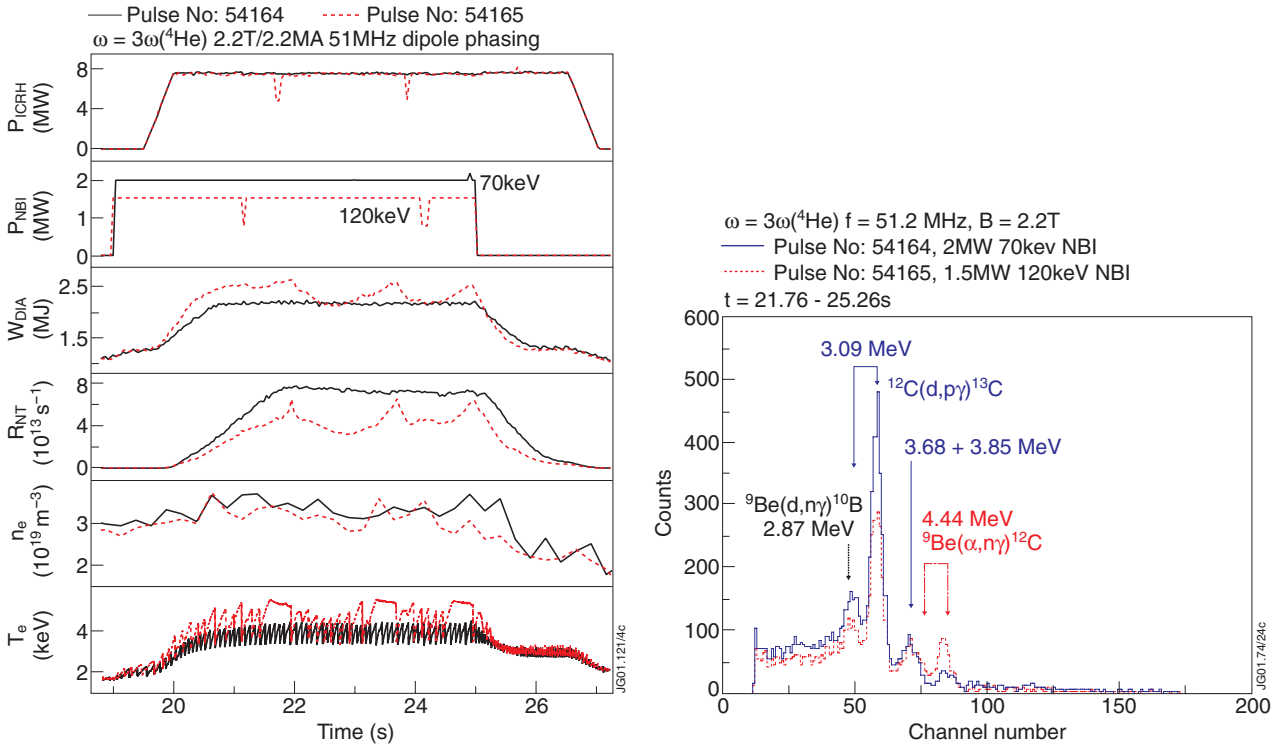

Figure 5: (a) Overview of Pulse No's: 54164 and 54165 with third harmonic ^{4}He heating and with 70keV and 120keV ^{4}He beams, respectively. (b) Gamma ray spectra for the two discharges.